Sensors and Materials, Vol. 33, No. 1 (2021) 241–250
MYU Tokyo

S & M 2450

Photolithography-free Vessel-on-a-chip to Simulate Tumor Cell Extravasation

Yuichiro Asaumi[1] and Naoki Sasaki[1,2*]

[1]Department of Applied Chemistry, Faculty of Science and Engineering, Toyo University,
2100 Kujirai, Kawagoe, Saitama 350-8585, Japan
[2]Department of Chemistry, College of Science, Rikkyo University,
3-34-1 Nishi-Ikebukuro, Toshima, Tokyo 171-8501, Japan

(Received September 30, 2020; accepted December 7, 2020)

Keywords: microfluidics, metastasis, migration, inhibitor, porous membrane

A photolithography-free vessel-on-a-chip (VOC) to simulate tumor cell extravasation is presented. A microfluidic device integrated with two pieces of porous membranes was fabricated without using photolithography. The directional migration of MDA-MB-231 cells, a metastatic tumor cell line, was observed in the presence of a concentration gradient of fetal bovine serum (FBS). Migration assays toward CXCL12 demonstrated the directional migration of the cells in the presence of a concentration gradient of chemokines. The migration was inhibited by pre-incubating the cells with AMD3100, a known inhibitor. Transendothelial migration assays with human umbilical vein endothelial cells cultured on the porous membrane revealed that there is a delay time prior to the migration of MDA-MB-231 cells through the endothelial cell layer. The present VOC will be utilized to clarify the mechanism of transendothelial migration of tumor cells as well as to screen antimetastatic drug candidates.

1. Introduction

Cancer is the leading cause of death in Japan.(1) More than 90% of these cancer deaths are due to metastasis.(2) Therefore, elucidating the mechanisms of cancer metastasis is important for the development of antimetastatic drugs.(2)

Extravasation is an important process in determining the metastatic destination of tumor cells. Tumor cells adhere to vascular walls, extravasate, invade the interstitium, and proliferate to form metastatic foci (Fig. 1). Many molecules are involved in extravasation, including transforming growth factor β(3) and adenosine triphosphate.(4) Furthermore, physical factors such as blood flow are also involved.(5) Thus, since various factors are involved in extravasation, it is necessary to consider the effects of each factor separately.

Chemokines have been recognized as one of the main factors that promote extravasation. Tumor cells expressing chemokine receptors receive chemokines on the cell surface and migrate. CXCR4, a type of chemokine receptor, is rarely expressed in normal cells, whereas it is highly expressed in primary tumor cells.(6) CXCR4 is also highly expressed in highly invasive cells.(7) Chemokine CXCL12 is highly expressed in organs that are the major metastatic sites of tumors.(6)

*Corresponding author: e-mail: n_sasaki@rikkyo.ac.jp
https://doi.org/10.18494/SAM.2021.3073

ISSN 0914-4935
https://myukk.org/

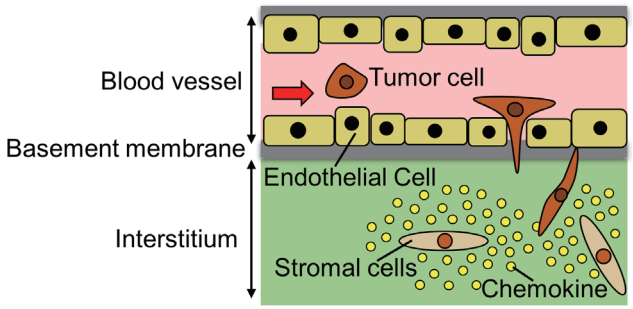

Fig. 1. (Color online) Schematic illustration of tumor cell extravasation.

Tumor cells stimulated by CXCL12 are known to change their actin skeleton and activate for migration within minutes of stimulation.[6,7] Therefore, the evaluation of the extravasation of tumor cells in the presence of CXCL12 and the identification of substances that inhibit the extravasation will lead to the development of new metastasis inhibitors targeting extravasation.

Microfluidic devices have been utilized to analyze the extravasation of tumor cells because of their advantages such as small sample/reagent consumption, compatibility with microscopic real-time observation, and the integration of multiple cell types onto the same device. Riahi *et al.* have reported a microfluidic device to examine the invasion capacity of MDA-MB-231 cells through an endothelial layer into Matrigel™ mixed with CXCL12.[8] Chaw *et al.* have analyzed the infiltration of MDA-MB-231 cells into Matrigel surrounded by fetal bovine serum (FBS) solution.[9] These methods allow the real-time observation of cell migration with small reagent consumption. However, because these methods use photolithography for device fabrication, they require specialized equipment and expensive reagents.

In this study, we present a photolithography-free vessel-on-a-chip (VOC) to simulate tumor cell extravasation (Fig. 2). We evaluate the effects of chemokines and inhibitors on the extravasation of tumor cells using the VOC. To do this, we first fabricate a microfluidic device integrated with two pieces of porous membranes. The membranes are inserted perpendicular to the device to facilitate the observation of cell migration through the membranes under a conventional epifluorescence microscope. Next, we demonstrate that the tumor cells seeded on a porous membrane can sense the concentration gradient of FBS and migrate. Furthermore, we evaluate the response of tumor cells to CXCL12 in the presence of AMD3100, a migration inhibitor. Finally, we seed vascular endothelial cells on a porous membrane and observe the invasion of tumor cells through the endothelial cell layer to evaluate the effect of the layer on the invasion.

2. Materials and Methods

2.1 Cells and culture procedures

MDA-MB-231 cells (ECACC, Public Health England, Salisbury, UK) were selected as a representative human metastatic tumor cell line. The cells were cultured in a 12.5 cm^2 cell

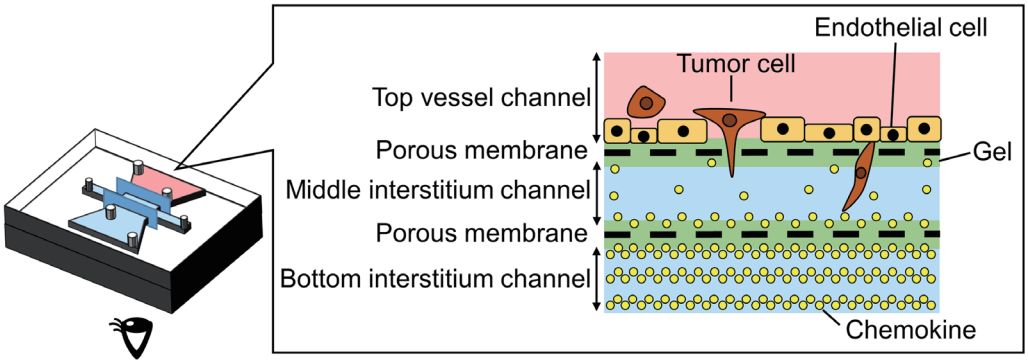

Fig. 2. (Color online) Concept of this study.

culture flask (353018, Becton, Dickinson and Company, Franklin Lakes, NJ, USA). The cells were grown in Dulbecco's modified Eagle's medium (DMEM, D6429, Sigma-Aldrich, St. Louis, MO, USA) supplemented with 10% FBS (S1820-500, Biowest, Nuaillé, France) and 1× antibiotic-antimycotic (15240-062, Thermo Fisher Scientific, Waltham, MA, USA). Phosphate-buffered saline (PBS) was prepared using PBS tablets (TAKARA BIO, Shiga, Japan).

Once cells reached confluence, the medium in a cell culture flask was aspirated. The cells were rinsed with 5 mL of PBS, and the PBS was aspirated. Then, 0.5 mL of TrypLE™ Express Enzyme (12604-013, Thermo Fisher Scientific) was added, and the flask was incubated for 3 min at 37 °C under an atmosphere of 5% CO_2 and 95% air. 1 mL of fresh medium was added to the flask and the obtained cell suspension was added to a 15 mL conical tube containing 4 mL of fresh medium. The tube was centrifuged at 1200 rpm for 4 min and the supernatant was aspirated. Finally, the cells were resuspended in the medium at the required concentration.

Human umbilical vein endothelial cells (HUVECs, C2519A, Lonza, Basel, Switzerland) were selected as a representative of normal human endothelial cells. HUVECs were cultured in a 25 cm^2 cell culture flask (3289, Corning, NY, USA). The cells were grown in Endothelial Cell Growth Medium 2 Kit (C-22111, PromoCell GmbH, Heidelberg, Germany).

2.2 Microfabrication

Schematic illustrations of the procedure of fabricating the microfluidic device are shown in Figs. 3(a)–3(g). An acrylic plate was cut out of an acrylic sheet (0.5 mm thickness, CLAREX, Nitto Jushi Kogyo, Tokyo, Japan) with a consumer laser cutter (HAJIME, Oh-Laser, Saitama, Japan) [Fig. 3(a)] and glued to another acrylic plate (1 mm thickness, CLAREX, Nitto Jushi Kogyo) with a glue (Acrysunday 14-3201, Acrysunday, Tokyo, Japan) to form a master for the top substrate [Fig. 3(b)].[10] A master for the bottom substrate (without a microchannel pattern) was fabricated in a similar manner. Poly(dimethylsiloxane) (PDMS) substrates were fabricated by pouring a prepolymer of PDMS (SILPOT 184, Dow Corning, Midland, MI, USA) on the master. The prepolymer was cured in an oven at 65 °C for 60 min, and the cured PDMS was

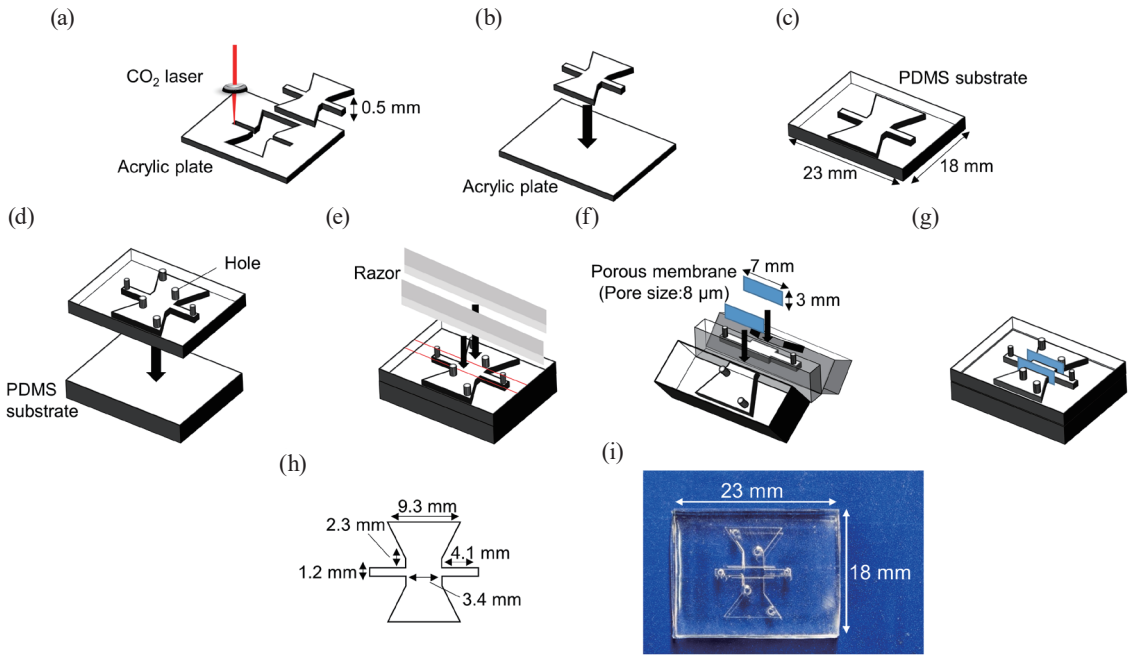

Fig. 3. (Color online) Schematic illustrations of procedure of fabricating photolithography-free VOC. (a) Cutting acrylic plate with CO_2 laser. (b) Bonding. (c) Molding. (d) Bonding and punching. (e) Cutting with razors to make crevices. (f) Inserting membranes. (g) Sealing. (h) Dimensions of channel. (i) Image of device.

peeled off from the master [Fig. 3(c)]. Through-holes were punched on the top substrate using metallic eyelets. The top and bottom substrates were plasma-treated (0.5 Torr, 80 W, 30 s) with a plasma cleaner (CUTE-MPQ(MP/R), FEMTO SCIENCE Inc., Korea), placed in contact with one another [Fig. 3(d)], and baked at 100 °C for 30 min. Porous polyethylene terephthalate membranes with a pore size of 8 μm were cut from cell culture inserts (353093, Becton, Dickinson and Company) to a size of 3 × 7 mm^2. Two crevices were formed on the bonded substrates by a razor [Fig. 3(e)], and the membranes were inserted into the crevices [Fig. 3(f)]. Afterward, the device was baked at 100 °C for 60 min to seal the crevices [Fig. 3(g)] with the help of the self-healing properties of PDMS, which contains unreacted curing agents.

2.3 Migration assays toward FBS

The microfluidic devices were placed in a clean bench on the day before the experiment and UV-sterilized overnight. On the day before the experiment, the medium in the flask in which the MDA-MB-231 cells were cultured was replaced with FBS-free DMEM to starve the cells.

The device was placed in a vacuum desiccator and degassed for 1 h. Matrigel (356234, Corning) with a known protein concentration of 9.1 mg/mL was thawed on an ice bath. 50 μL of Matrigel was mixed with 2.225 mL of 10 mM Tris-HCl (pH 8.0)/0.7% NaCl solution to make 200 μg/mL Matrigel solution. The prepared Matrigel solution was introduced into all channels of the device and incubated in an incubator for 1 h.

CellTracker (CellTracker Green CMFDA Dye, C7025, Thermo Fisher Scientific) was used to label the cells. A staining solution containing 1 μM CellTracker in DMEM was used. The medium in the flask was aspirated. 5 mL of the staining solution was added to the flask and incubated in an incubator for 30 min to prepare a stained cell suspension (10^6 cells/mL). The cell suspension was introduced into the top vessel channel of the device, and DMEM was introduced into the interstitium channels. The device was sealed with a PDMS slab and placed in a wet box vertically with the top vessel channel up for 3–4 h in an incubator to allow the cells to adhere to the membrane. To create a concentration gradient of FBS, firstly, DMEM was removed from the interstitium channels. Then, DMEM was introduced into the middle interstitium channel shown in Fig. 2, and DMEM containing 10% FBS was introduced into the bottom interstitium channel. Control experiments were conducted by introducing DMEM containing 10% FBS into all the channels.

Fluorescence time-lapse imaging was conducted using an inverted microscope (CKX53, OLYMPUS, Tokyo, Japan) equipped with a 100 W high-pressure mercury lamp, a 10× objective lens (NA 0.30), a CMOS camera (CS2100M-USB, Thorlabs Japan, Tokyo, Japan), a shutter controller (SSH-C4B, Sigma Koki, Tokyo, Japan), and a stage top incubator (INU-ONICS-F1, Tokai Hit, Shizuoka, Japan). A 35 mm dish (3000-035, AGC Inc., Tokyo, Japan) on which the device was placed was filled with sterilized water, and the dish was placed in the stage top incubator. The camera and the shutter were controlled using Micro-manager 1.4.23[11] and processed using image analysis software (Image J 1.52v, National Institutes of Health, Bethesda, MD, USA).

2.4 Migration assays toward CXCL12

The experimental procedure was the same as in Sect. 2.3 except for some modifications described below. MDA-MB-231 cells were not starved. Matrigel (356237, Corning) with a known protein concentration of 10.5 mg/mL was used. The final concentration of the Matrigel solution was 300 μg/mL. A stained cell suspension was prepared with DMEM containing 1% BSA. The cell suspension was introduced into the top vessel channel of the device, and DMEM containing 1% BSA was introduced into the interstitium channels. After 3 h of incubation, DMEM containing 1% BSA was removed from the interstitium channels. Then, DMEM was introduced into the middle interstitium channel shown in Fig. 2, and 100 ng/mL CXCL12 (300-28A, Peprotech Inc., Cranbury, NJ, USA) in DMEM was introduced into the bottom interstitium channel. Control experiments were conducted by introducing DMEM into all the channels.

Inhibitor assay on the device was demonstrated using AMD3100, a well-known CXCR4 antagonist.[12] MDA-MB-231 cells were incubated with 25 μg/mL AMD3100 (A5602, Sigma-Aldrich) in DMEM for 30 min and employed for assay.

2.5 Transendothelial migration assays

The experimental procedure was the same as in Sect. 2.4 except for some modifications described below. After incubating the device filled with 300 μg/mL Matrigel solution, the

solution was removed and all channels were washed twice with the medium for HUVECs. A suspension of HUVECs (10^7 cells/mL) was introduced into the top vessel channel, and the medium for HUVECs was introduced into the interstitium channels. The device was incubated not for 3 h but for 1 day to form an artificial endothelium on the membrane. The endothelialized device was employed for transendothelial migration assays.

3. Results and Discussion

3.1 Microfluidic device

Figure 3(h) shows the dimensions of the microchannel. The microchannel was designed so as to integrate two pieces of porous membranes perpendicular into the device and to enable the observation of tumor cell migration through the membrane or artificial endothelium created by HUVECs on the membrane. A typical image of the device is shown in Fig. 3(i). The device was successfully fabricated without solution leakage.

Note that the fabrication of the thick master for the deep (0.5 mm) microchannel is difficult with conventional spin coating and photolithography. The deep microchannel has an advantage in minimizing the effects of evaporation through the PDMS substrates and allows us to perform cell culture and cell migration assays successfully.

3.2 Migration assays toward FBS

Fluorescence images of MDA-MB-231 cells migrated toward FBS in a microchannel are shown in Fig. 4. In the absence of an FBS concentration gradient, few MDA-MB-231 cells migrated across the porous membrane (data not shown), whereas in the presence of an FBS concentration gradient, a large number of MDA-MB-231 cells migrated into the middle interstitium channel [Fig. 4(b)].

Figure 5 shows the trajectory of cell migration and circular histograms. In the presence of an FBS concentration gradient, the cells migrated downward, which clearly shows the directional

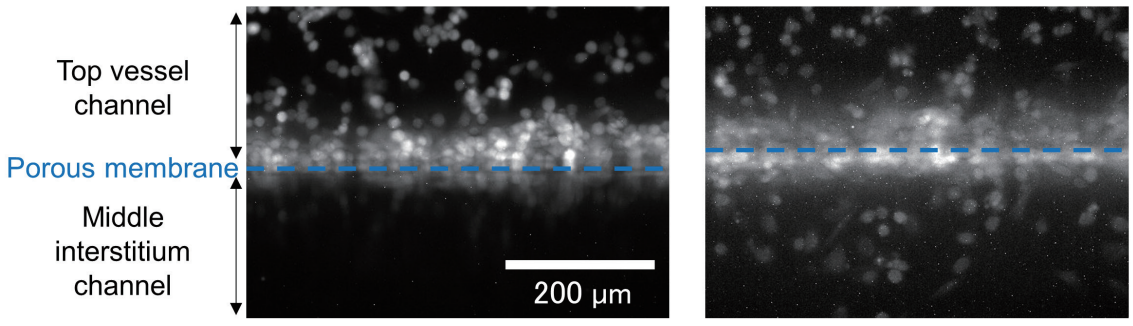

Fig. 4. (Color online) Fluorescence images of migration assay toward FBS: (a) 0 and (b) 24 h.

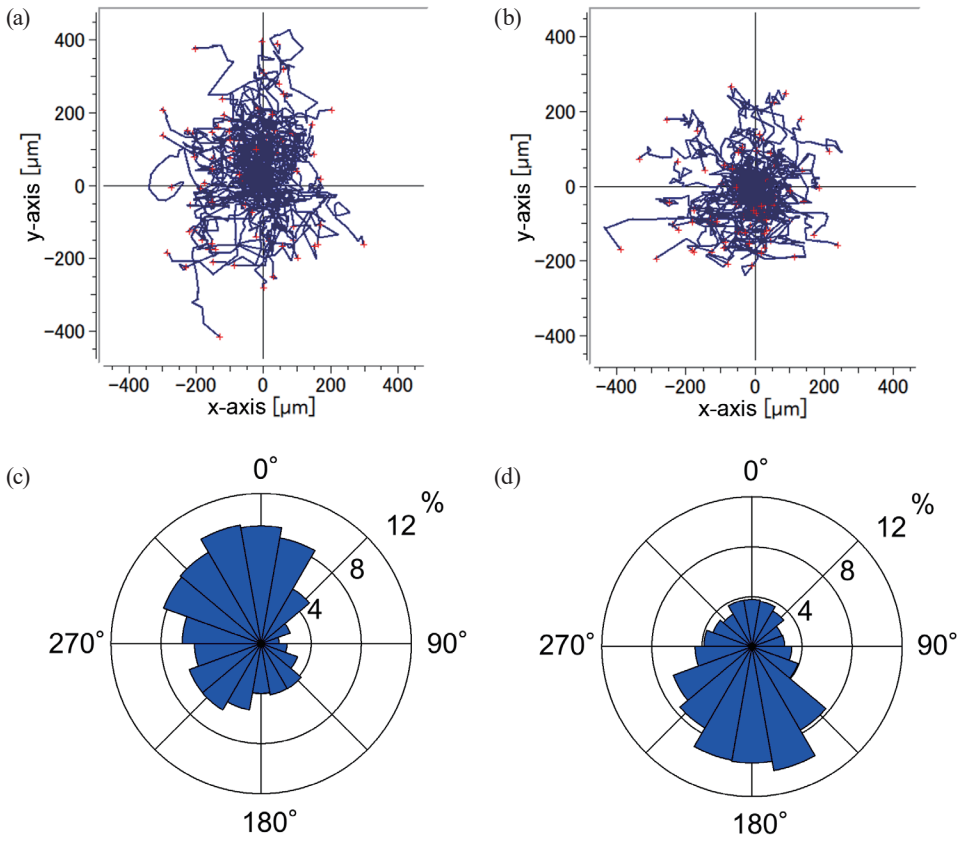

Fig. 5. (Color online) (a, b) Trajectories of tumor cells. Plotted tracks were superimposed at (0,0) in the (a) absence and (b) presence of FBS concentration gradient. (c, d) Circular histograms of tumor cell migrationin the (c) absence and (d) presence of FBS concentration gradient. Interior angle = 60°, range interval = 20°, and $N = 75$.

migration of the cells. In the absence of an FBS concentration gradient, the cells migrated upward, suggesting that they were densely packed near the membrane and migrated upward where there was a space.

3.3 Migration assays toward CXCL12

Fluorescence images of MDA-MB-231 cells that migrated toward CXCL12 in a microchannel are shown in Fig. 6. A number of cells migrated into the middle interstitium channel. After 24 h of observation, most of the cells had curled up, suggesting that the cells were in poor condition. Therefore, we limited the duration of the observation to 18 h. The normalized migration number, which indicates how many cells migrated, was calculated as the ratio of the number of cells in the middle interstitium channel to that in the top vessel channel. Figure 7 shows the relationship between the normalized migration number and time. There is a significant difference between the data of control experiments and that of experiments with CXCL12. This result demonstrates the induction of directional tumor cell migration by CXCL12.

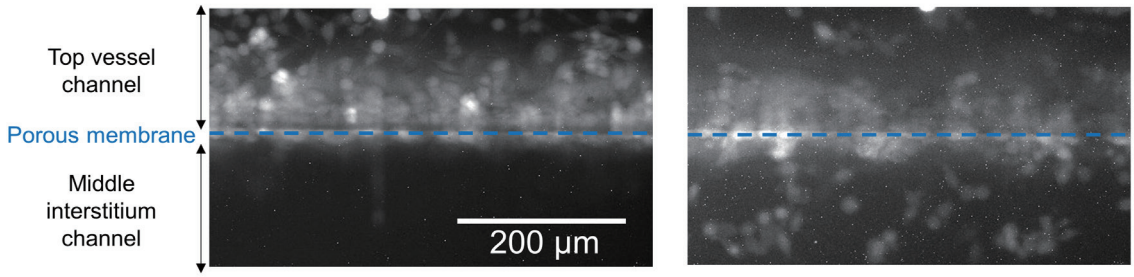

Fig. 6. (Color online) Fluorescence images of migration assay toward CXCL12: (a) 0 and (b) 18 h.

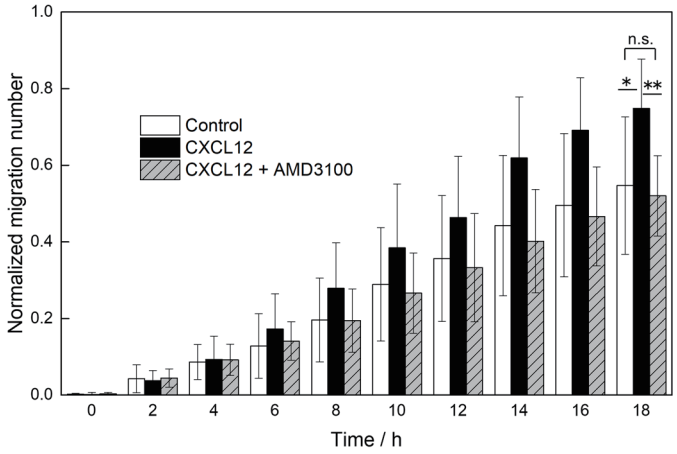

Fig. 7. Time courses of normalized migration number in the absence of CXCL12 (white bars), in the presence of CXCL12 (black bars), and in the presence of CXCL12 using cells pre-incubated with AMD3100 (hatched bars). *$P < 0.05$, **$P < 0.01$. Error bars indicate ±1 SD of six experiments.

Figure 7 also shows the normalized migration number of cells pre-incubated with AMD3100. There is no significant difference between the data of the control experiments and that of the experiments with AMD3100. This result demonstrates the inhibition of directional tumor cell migration by AMD3100. In addition, we calculated the ratio of the migration number without and with the addition of AMD3100. The ratio was 1:0.70, which was close to a reported value (1:0.71).[12] Therefore, the present results are consistent with those in previous reports.

3.4 Transendothelial migration assays

Fluorescence images of MDA-MB-231 cells migrated toward CXCL12 through the artificial endothelium (HUVEC layer on the membrane) are shown in Fig. 8. After 12 h of incubation, the cells had hardly migrated. In contrast, after 24 h of incubation, the cells had migrated to the middle interstitium channel across the HUVEC layer. The number of migrated cells at 24 h was 57 ± 57, which was clearly smaller than that in the absence of HUVECs (182 ± 28). Therefore, the presence of the HUVEC layer on the membrane was confirmed.

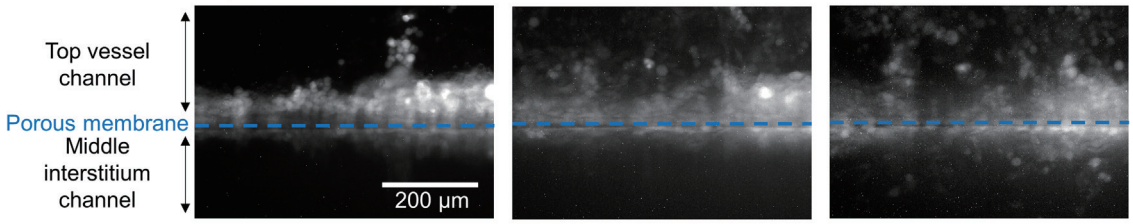

Fig. 8. (Color online) Fluorescence images of transendothelial migration assay. (a) 0 h. (b) 12 h. (c) 24 h.

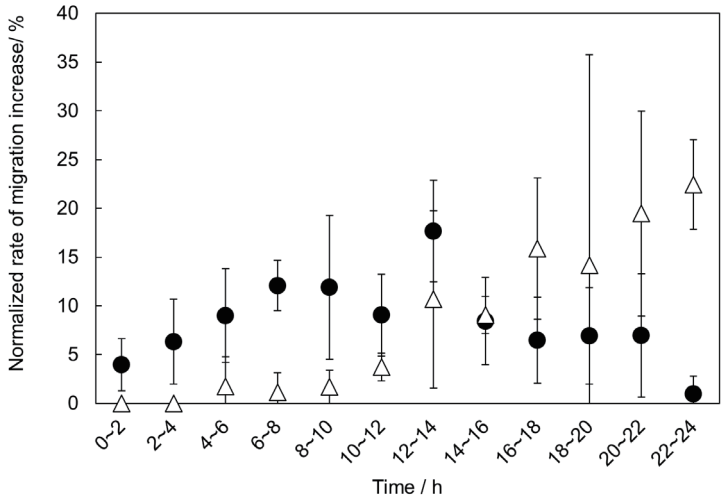

Fig. 9. Time course of normalized rate of migration increase in the absence of HUVECs (filled circles) and in the presence of HUVECs (open triangles). Error bars indicate ±1 SD of six experiments (in the absence of HUVECs) and three experiments (in the presence of HUVECs).

Figure 9 shows the relationship between the normalized rate of migration increase and the time for the migration assays in the absence and presence of HUVECs. The normalized rate of migration increase was calculated by dividing the number of migrated cells at each time duration by the number of migrated cells at 24 h. This value indicates how much the number of migrated cells increased at each time duration. As shown in Fig. 9, a substantial difference was observed between the time courses. These results indicate that MDA-MB-231 cells required at least 10 h to cross the HUVEC layer. Also, MDA-MB-231 cells may have changed their cell morphology and crept between the HUVEC junctions, or the MDA-MB-231 cells may have secreted some factor that broke the intercellular junctions between the HUVECs and migrated. These results suggest that this device can be used to assess the invasion of tumor cells into vascular endothelial cells in a shorter time with a higher spatial resolution than in the case of the conventional evaluation of tumor cell invasion into vascular endothelial cells using culture inserts.

4. Conclusions

We have developed a photolithography-free VOC to simulate tumor cell extravasation. By using the VOC, it is possible to evaluate the effects of chemokines, vascular endothelial cells, and inhibitors on the extravasation of tumor cells. Our VOC will contribute to drug screening for the development of new metastasis inhibitors. In addition, by applying a solution flow, we expect the evaluation of tumor cell migration under *in vivo*-like flow conditions.

Acknowledgments

This work was supported in part by The INOUE ENRYO Memorial Grant, Toyo University.

References

1 Ministry of Health, Labour and Welfare, Japan: Trends in Leading Causes of Death, https://www.mhlw.go.jp/english/database/db-hw/populate/dl/E03.pdf (accessed September 2020).
2 X. Guan: Acta Pharm. Sin. B **5** (2015) 402. https://doi.org/10.1016/j.apsb.2015.07.005
3 B. Strilic and S. Offermanns: Cancer Cell **32** (2017) 282. https://doi.org/10.1016/j.ccell.2017.07.001
4 D. Schumacher, B. Strilic, K. K. Sivaraj, N. Wettschureck, and S. Offermanns: Cancer Cell **24** (2013) 130. https://doi.org/10.1016/j.ccr.2013.05.008
5 G. Follain, N. Osmani, A. S. Azevedo, G. Allio, L. Mercier, M. A Karreman, G. Solecki, M. J. G. Leòn, O. Lefebvre, N. Fekonja, C. Hille, V. Chabannes, G. Dollé, T. Metivet, F. D. Hovsepian, C. Prudhomme, A. Pichot, N. Paul, R. Carapito, S. Bahram, B. Ruthensteiner, A. Kemmling, S. Siemonsen, T. Schneider, J. Fiehler, M. Glatzel, F. Winkler, Y. Schwab, K. Pantel, S. Harlepp, and J. G Goetz: Dev. Cell **45** (2018) 33. https://doi.org/10.1016/j.devcel.2018.02.015
6 A. Müller, B. Homey, H. Soto, N. Ge, D. Catron, M. E. Buchanan, T. McClanahan, E. Murphy, W. Yuan, S. N. Wagner, J. L. Barrera, A. Mohar, E. Verástegui, and A. Zlotnik: Nature **410** (2001) 50. https://doi.org/10.1038/35065016
7 P. Gassmann, J. Haier, K. Schlüter, B. Domikowsky, C. Wendel, U. Wiesner, R. Kubitza, R. Engers, S. W Schneider, B. Homey, and A. Müller: Neoplasia **11** (2009) 651. https://doi.org/10.1593/neo.09272
8 R. Riahi, Y. L. Yang, H. Kim, L. Jiang, P. K. Wong, and Y. Zohar: Biomicrofluidics **8** (2014) 024103. https://doi.org/10.1063/1.4868301
9 K. C. Chaw, M. Manimaran, F. E. H. Tay, and S. Swaminathan: Biomed. Microdevices **9** (2007) 597. https://doi.org/10.1007/s10544-007-9071-5
10 N. Sasaki, K. Tsuchiya, and H. Kobayashi: Sens. Mater. **31** (2019) 107. https://doi.org/10.18494/SAM.2019.2125
11 A. D. Edelstein, M. A. Tsuchida, N. Amodaj, H. Pinkard, R. D. Vale, and N. Stuurman: J. Biol. Methods **1** (2014) e10. http://dx.doi.org/10.14440/jbm.2014.36
12 U. M. Domanska, H. T.-Bosscha, W. B. Nagengast, T. H. O. Munnink, R. C. Kruizinga, H. J. K. Ananias, N. M. Kliphuis, G. Huls, E. G. E. De Vries, I. J. de Jong, and A. M. E. Walenkamp: Neoplasia **14** (2012) 709. https://doi.org/10.1593/neo.12324